SCIENCE CHINA
Technological Sciences

• Article •

April 2021 Vol. 64 No. 4: 836–846
https://doi.org/10.1007/s11431-020-1671-6

Iterative assist-as-needed control with interaction factor for rehabilitation robots

CAO Ran[1,2], CHENG Long[1,2*], YANG ChenGuang[3] & DONG Zhe[4]

[1]*School of Artificial Intelligence, University of Chinese Academy of Sciences, Beijing 100049, China;*
[2]*State Key Laboratory for Management and Control of Complex Systems, Institute of Automation, Chinese Academy of Sciences, Beijing 100190, China;*
[3]*School of Automation Science and Engineering, South China University of Technology, Guangzhou 510641, China;*
[4]*School of Electrical and Control Engineering, North China University of Technology, Beijing 100144, China*

Received April 20, 2020; accepted June 4, 2020; published online January 18, 2021

Rehabilitation robots for stroke patients have drawn considerable attention because they can reduce the economic and labor costs brought by traditional rehabilitation. Control methods for rehabilitation robots have been developed to stimulate the active motion of patients and to improve the effectiveness of rehabilitation care. However, current control methods can only roughly adjust the system's stiffness and may fail in achieving satisfactory performance. To this end, this paper introduces a novel cost function consisting of the tracking error term and the stiffness term. The cost function contains an interaction factor that represents the patient's motion intention to balance the weight of these two terms. When the patients try to actively do training tasks, the weight of stiffness term increases, which leads to the larger allowable tracking error and lower stiffness eventually. An iterative updating law of the stiffness matrix is given to reduce the proposed cost function. Theoretical analysis based on the Lyapunov theory is given to ensure the feasibility of the proposed algorithm. Furthermore, a force estimation is used to improve interaction control performance. Finally, simulation experiments are provided to show the effectiveness of the proposed algorithm.

Keywords: human-robot interaction, impedance, stiffness, control, rehabilitation

Citation: Cao R, Cheng L, Yang C G, et al. Iterative assist-as-needed control with interaction factor for rehabilitation robots. Sci China Tech Sci, 2021, 64: 836–846, https://doi.org/10.1007/s11431-020-1671-6

1 Introduction

It has been reported that the number of stroke patients aged 40 and over in China has increased to 12.42 million. 70% of stroke patients suffer from the effect of disability [1]. Rehabilitation of stroke patients usually needs long-term help from physical therapists, which brings a heavy economic burden for those patients. Meanwhile, the gap between the numbers of patients and physical therapists has limited the available rehabilitation care [2]. To solve this issue, rehabilitation robots have been used to assist the repetitive rehabilitation training tasks. The main design methodology of the rehabilitation robot includes the platform type robot and the exoskeleton type robot. The exoskeleton type robot needs to be worn on the patient's body, which applies few constraints on the patient's ordinary movement. There are considerable applications of the exoskeleton type robot in the area of the rehabilitation, i.e., the upper limb exoskeleton, lower limb exoskeleton and hand exoskeleton [3–5]. The platform type robot is fixed on the stationary platform rather than putting on the patient's body. Hence the platform type robot can bring a lower burden than the exoskeleton based robot. One typical application of the platform type robot is the ankle rehabilitation robot [6–9]. Different from other robots [10–13], there exist a large amount of interactions during the rehabilitation training. Therefore, the safe and efficient interactive control

*Corresponding author (email: long.cheng@ia.ac.cn)

becomes one key issue of the rehabilitation robot.

For guaranteeing the compliant physical interaction between robots and a variety of environments, impedance control has been adopted for the interaction control during the past thirty years [14, 15]. Impedance control aims at keeping the desired force relationship between the robot and the environment [16, 17]. As a special implementation of the impedance control, the admittance control calculates the desired reference trajectory from the desired interaction relationship and the measured interaction force, and the desired reference trajectory is then tracked by using the position tracking controller. When the environment is unknown, some adaptive impedance/admittance controllers have been adopted by using the optimal control methods or the adaptive control methods [18–20]. For example, in ref. [21], the authors designed a fuzzy logic based gain regulator to implement the adaptive admittance control which is applied on a redundantly actuated ankle rehabilitation robot. However, when the environment is time-varying, designing one appropriate impedance controller still faces grand challenges.

Towards this challenge, iterative learning control has been used in this area [22]. Iterative learning control can adjust the stiffness parameter trial after trial during repetitive tasks. For tackling the situation that the interaction force may be different in each trial (i.e., in a human-robot interaction), a control law motivated by the human central nervous system was proposed [23]. In this human-like control method, an iterative adaptive law was designed to minimize the tracking error and the stiffness term (the difference of the desired stiffness and the controller stiffness). Furthermore, a robot controller adapting the stiffness and reference trajectory simultaneously and a bio-inspired controller imitating human motor learning properties were provided for the interaction with the time-varying environment [24, 25]. However, in a rehabilitation training scenario, iterative learning control only focuses on how to adjust the controller to ensure the convergence of the system's state as well as the interaction force. It cannot stimulate the active participation of the patients, which limits its usage in rehabilitation.

To overcome this limitation, an idea of "assist-as-needed (AAN) control" has been proposed in ref. [26], which considers the fact that stimulating the patient's motion intention is helpful to his/her recovery [27]. With the AAN controller, the robot only gives the needed force when the patient's functional capability is not sufficiently strong to complete the training tasks. When the patients can drive the robot to complete tasks, the robot system should be compliant and follow the motion of the patient. To achieve this idea, a minimal controller was designed for the upper limb rehabilitation [28]. The designed controller consists of a sensor-less force observer and an impedance controller. The stiffness parameter of the impedance controller is iteratively updated by the designed updating law, and the stiffness parameter is adjusted with respect to the rehabilitation task's motion error. When the patients try to move actively and the motion error is greater than the desired value, the stiffness parameter decreases and the ultimate bound of the allowable tracking error increases, vice versa. From another view of achieving the AAN control, an adaptive human-robot interaction control based on the series elastic actuator (SEA) was proposed in refs. [29, 30]. The designed control method divided the control mode into the robot-in-charge mode and the human-in-charge mode. A smooth switching law was given to guarantee the stability of the whole system. However, these controllers cannot minimize tracking errors and stiffness terms, which leads to a worse performance compared with the aforementioned iterative learning control.

In this paper, a novel iterative adaptive control method is proposed to achieve the AAN controller. First, a novel cost function with an interaction factor is proposed to balance the weight of the tracking error and the stiffness term. The interaction factor in this paper is designed according to the interaction force. However, any other measured signals that can reflect the patient's motion intention can be used to determine the interaction factor (i.e., the tracking error or the surface electromyography (sEMG) [31]). A larger interaction factor caused by the strong motion intention leads to the higher weight of the stiffness item, which means that the algorithm tends to reduce the stiffness term rather than the tracking error. Hence, the performance of the whole system can be adaptively adjusted according to the patient's motion intention. An iterative updating law of the stiffness matrix is given to reduce the cost function. The ultimate bounded set of the tracking error and the stiffness parameter is analyzed based on the Lyapunov theory. The main contributions and innovations of this paper are listed as follows.

(1) A novel cost function with an interaction factor is given, and this interaction factor represents the motion intention and affects the weight of each term in the cost function.

(2) An appropriate iterative updating law is designed to reduce the proposed cost function. The allowable bounded set of the ultimate tracking error and stiffness parameters are theoretically analyzed.

(3) The controller with a force estimation is presented to further improve the performance of the whole system.

2 Methodology

2.1 System model

In this paper, the dynamic model of the rehabilitation robot

can be written by the following Euler-Lagrange equation:

$$M(q)\ddot{q} + C(q,\dot{q})\dot{q} + G(q) = \tau_c + \tau_i, \tag{1}$$

where q, $\dot{q}$ and $\ddot{q}$ denote the joint position, velocity and acceleration, respectively. $M(q)$ and $C(q,\dot{q})$ denote the inertia matrix and the Coriolis fore matrix, respectively. $G(q)$ is the gravity vector. τ_c and τ_i denote the control torque and the interaction torque with the patient, respectively. One common property of Euler-Lagrange dynamics is listed as follows [32].

Property 1. The matrix $\dot{M}_i(q_i(t)) - 2C_i(q_i(t),\dot{q}_i(t))$ is skew-symmetric.

Define a state variable s as follows:

$$\begin{aligned} q_e &= q - q_d, \\ s &= \dot{q}_e + q_e, \end{aligned} \tag{2}$$

where q_d is the desired rehabilitation task trajectory. q_e and $\dot{q}_e$ denote the position error and the velocity error with respect to the desired trajectory, respectively. s represents the filtered tracking error, which is usually used in the design of robot controller [33]. It can be proven that s goes to zero if and only if q_e goes to zero.

The following impedance controller combined with the error feedback and the compensation of the system dynamics is adopted:

$$\tau_c = -K(t)s + M(q)(\ddot{q}_d - \dot{q}_e) + C(q,\dot{q})(\dot{q}_d - q_e) + G(q), \tag{3}$$

where $K(t)$ is the stiffness matrix and it reflects the relationship between the tracking error and the control torque. A greater $K(t)$ means that the same tracking error can lead to a greater control torque, which makes the robotic system more "stiff". For rehabilitation tasks, choosing an appropriate stiffness parameter is difficult due to the different rehabilitation situation of the patients. To solve this problem, this paper uses the iterative algorithm to find the proper stiffness parameter in the next subsection.

2.2 Iterative adaptive control law

A cost function for minimizing the tracking error and the stiffness matrix is given as follows:

$$V(t) = V_p(t) + V_c(t), \tag{4}$$

where

$$\begin{aligned} V_p(t) &= \frac{1}{2}s^{\mathrm{T}}M(q)s, \\ V_c(t) &= \frac{1}{2}\int_{t-T}^{t} w_i^2 \mathrm{vec}(K(\tau))^{\mathrm{T}}\mathrm{vec}(K(\tau))\mathrm{d}\tau, \end{aligned}$$

and $\mathrm{vec}(\cdot)$ denotes the column vectorization operator. T is the interval length of every training trial. w_i is the interaction factor used to denote the human motion intention. In this paper, the interaction force is used to construct w_i as follows:

$$w_i = \frac{1}{1 + \mathrm{e}^{-(\overline{\tau}_i^{k-1} - \tau^*)}},$$

where $\overline{\tau}_i^{k-1}$ represents the mean value of interaction force in the $(k-1)$th training trial and τ^* denotes the desired interaction force determined by the patient's rehabilitation condition. In practice, the desired interaction force can be directly obtained by recording the interaction force between the patient and the experienced therapist during the manual rehabilitation training. The interaction factor follows the formula of the sigmoid function which maps the interaction force to a value within the interval $(0,1)$. In fact, any monotone and smooth function ranged from $(0,1)$ can be considered as a candidate function for the interaction factor.

Remark 1. The reason of minimizing $V_p(t)$ is to reduce the tracking error during the ith training trial. The reason of minimizing $V_c(t)$ is that a smaller $K(t)$ can lead to a "less" intervention from the rehabilitation robot, which stimulates the active participation of patients. Therefore, the cost function defined by eq. (4) is expected to be minimized.

Define an auxiliary variable $X(t) = w_i\mathrm{vec}(K(t))$. Rewrite $V_c(t)$ to be $V_c(t) = \frac{1}{2}\int_{t-T}^{t} X^{\mathrm{T}}(\tau)X(\tau)\mathrm{d}\tau$. To reduce the cost function defined by eq. (4), an iterative updating law of $X(t)$ is proposed as follows:

$$\delta X(t) = X(t) - X(t-T) = \mathrm{vec}(ss^{\mathrm{T}}) - \frac{\gamma}{1-w_i}X(t), \tag{5}$$

where $\gamma > 0$ denotes the forgetting factor. Note that eq. (5) can be rewritten as

$$X(t) = \frac{1-w_i}{1+\gamma-w_i}[\mathrm{vec}(ss^{\mathrm{T}}) + X(t-T)]. \tag{6}$$

Taking the fact that $X(t) = w_i\mathrm{vec}(K(t))$ into eq. (6) can obtain the iterative updating law of $K(t)$:

$$\mathrm{vec}(K(t)) = \frac{1-w_i}{(1+\gamma-w_i)w_i}[\mathrm{vec}(ss^{\mathrm{T}}) + w_{i-1}\mathrm{vec}(K(t-T))]. \tag{7}$$

Lemma 1. The stiffness matrix $K(t)$ in eq. (7) is always symmetric positive definitive if $K(t)$, $k \in [0,T)$ is symmetric positive definitive.

Proof. For the first iteration, it follows form eq. (7) that $K(t) = \frac{1-w_i}{(1+\gamma-w_i)w_i}[\mathrm{vec}(ss^{\mathrm{T}}) + w_{i-1}\mathrm{vec}(K(t-T))]$, $t \in [T,2T)$. Since $s^{\mathrm{T}}s$ is symmetric positive semi-definitive, $K(t)$ $(t \in [0,T))$ is symmetric positive definitive and $0 < w_i < 1$, it is easy to verify that $K(t)$ $(t \in [T,2T))$ is symmetric positive definitive. By repeating the same procedure, the correctness of this lemma can be proven.

Because the stiffness matrix $K(t)$ is always positive definitive, its minimal eigenvalue $\overline{\lambda}_K$ is positive.

The entire control block diagram of the proposed "assist-as-needed" controller is given in Figure 1. The iterative adaptive law uses the state information and the interaction force to generate the new stiffness matrix. Then the impedance controller uses the updated stiffness matrix and the tracking error to calculate the control force. Driven by the obtained control force, the robot system tracks the desired rehabilitation trajectory and keeps an impedance relationship with the patient.

Theorem 1. Under the iterative updating law defined by eq. (5) and the controller defined by eq. (3), the first-order difference of overall cost function satisfies that $\sigma V(t) = V(t) - V(t-T) \leq 0$ until $\|s\|$ and $\|\mathrm{vec}(K(t))\|$ ultimately go to a bounded set Ω defined in the following proof, which means that eqs. (3) and (5) lead to the decrease of eq. (4).

Proof. Taking eq. (3) into eq. (1) leads to

$$\begin{aligned} M(q)\ddot{q} + C(q,\dot{q})\dot{q} + G(q) &= -K(t)s + M(q)(\ddot{q}_\mathrm{d} - \dot{q}_\mathrm{e}) \\ &\quad + C(q,\dot{q})(\dot{q}_\mathrm{d} - q_\mathrm{e}) + G(q) + \tau_\mathrm{i}, \\ M(q)\dot{s} + C(q,\dot{q})s + K(t)s &= \tau_\mathrm{i}. \end{aligned} \tag{8}$$

Using Property 1, then the time-derivative of $V_p(t)$ can be written as

$$\begin{aligned} \dot{V}_p &= s^\mathrm{T}M(q)\dot{s} + \frac{1}{2}s^\mathrm{T}\dot{M}(q)s \\ &= s^\mathrm{T}[-C(q,\dot{q})s - K(t)s + \tau_i] + \frac{1}{2}s^\mathrm{T}\dot{M}(q)s \\ &= -s^\mathrm{T}K(t)s + s^\mathrm{T}\tau_i. \end{aligned} \tag{9}$$

Integrating eq. (9) from t to $(t-T)$, the first-order difference of $V_p(t)$ can be obtained:

$$\begin{aligned} \delta V_p &= V_p(t) + V_p(t-T) \\ &= \int_{t-T}^{t} \dot{V}_p(\tau)\mathrm{d}\tau \\ &= -\int_{t-T}^{t} (s^\mathrm{T}K(t)s - s^\mathrm{T}\tau_i)\mathrm{d}\tau. \end{aligned} \tag{10}$$

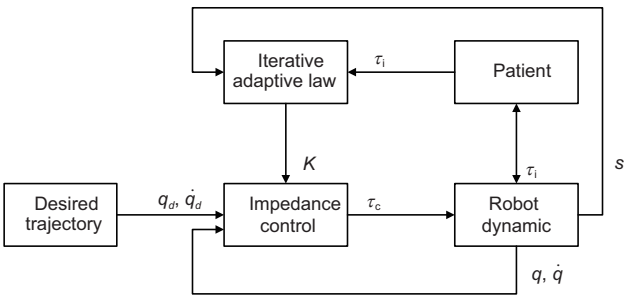

Figure 1 Control block diagram of the proposed "assist-as-needed" controller.

Next, the first-order difference of $V_\mathrm{c}(t)$ can be written as

$$\begin{aligned} \delta V_c &= V_\mathrm{c}(t) - V_\mathrm{c}(t-T) \\ &= \frac{1}{2}\int_{t-T}^{t} X^\mathrm{T}(\tau)X(\tau) - X(\tau-T)^\mathrm{T}X(\tau-T)\mathrm{d}\tau \\ &= \frac{1}{2}\int_{t-T}^{t} [X(\tau) - X(\tau-T)]^\mathrm{T}[X(\tau) + X(\tau-T)]\mathrm{d}\tau \\ &= \frac{1}{2}\int_{t-T}^{t} [X(\tau) - X(\tau-T)]^\mathrm{T}[2X(\tau) - X(\tau) + X(\tau-T)]\mathrm{d}\tau \\ &= -\frac{1}{2}\int_{t-T}^{t} (\delta X(\tau))^\mathrm{T}\delta X(\tau)\mathrm{d}\tau + \int_{t-T}^{t} (\delta X(\tau))^\mathrm{T}X(\tau)\mathrm{d}\tau. \end{aligned} \tag{11}$$

Taking eq. (5) into eq. (11), it can be obtained that

$$\begin{aligned} \delta V_c &= \int_{t-T}^{t} [\mathrm{vec}(ss^\mathrm{T}) - \frac{\gamma}{1-w_\mathrm{i}}X(\tau)]^\mathrm{T}X(\tau)\mathrm{d}\tau \\ &\quad - \frac{1}{2}\int_{t-T}^{t} \delta X(\tau)^\mathrm{T}\delta X(\tau)\mathrm{d}\tau \\ &= -\frac{1}{2}\int_{t-T}^{t} \delta X(\tau)^\mathrm{T}\delta X(\tau)\mathrm{d}\tau - \int_{t-T}^{t} \frac{\gamma}{1-w_\mathrm{i}}X(\tau)^\mathrm{T}X(\tau)\mathrm{d}\tau \\ &\quad + \int_{t-T}^{t} w_\mathrm{i}\mathrm{vec}(ss^\mathrm{T})^\mathrm{T}\mathrm{vec}(K(\tau))\mathrm{d}\tau \\ &= -\frac{1}{2}\int_{t-T}^{t} \delta X(\tau)^\mathrm{T}\delta X(\tau)\mathrm{d}\tau - \int_{t-T}^{t} \frac{\gamma}{1-w_\mathrm{i}}X(\tau)^\mathrm{T}X(\tau)\mathrm{d}\tau \\ &\quad + \int_{t-T}^{t} w_i s^\mathrm{T}K(\tau)s\mathrm{d}\tau. \end{aligned} \tag{12}$$

Combining eq. (10) and eq. (12) leads to

$$\begin{aligned} \delta V &= \delta V_\mathrm{c} + \delta V_p \\ &= -\frac{1}{2}\int_{t-T}^{t} \delta X(\tau)^\mathrm{T}\delta X(\tau)\mathrm{d}\tau - \int_{t-T}^{t} \frac{\gamma}{1-w_\mathrm{i}}X(\tau)^\mathrm{T}X(\tau)\mathrm{d}\tau \\ &\quad + \int_{t-T}^{t} w_i s^\mathrm{T}K(\tau)s\mathrm{d}\tau - \int_{t-T}^{t} (s^\mathrm{T}K(t)s - s^\mathrm{T}\tau_i)\mathrm{d}\tau \\ &= -\int_{t-T}^{t} [(1-w_\mathrm{i})s^\mathrm{T}Ks + \frac{\gamma}{1-w_\mathrm{i}}X(\tau)^\mathrm{T}X(\tau) - s^\mathrm{T}\tau_i]\mathrm{d}\tau \\ &\quad - \frac{1}{2}\int_{t-T}^{t} \delta X(\tau)^\mathrm{T}\delta X(\tau)\mathrm{d}\tau. \end{aligned} \tag{13}$$

Obviously, one sufficient condition to make $\delta V \leq 0$ is that

$$\begin{aligned} (1-w_\mathrm{i})s^\mathrm{T}Ks + \frac{\gamma}{1-w_\mathrm{i}}X(\tau)^\mathrm{T}X(\tau) - s^\mathrm{T}\tau_i &\geq (1-w_\mathrm{i})\overline{\lambda}_K\|s\|^2 \\ + \frac{\gamma}{1-w_\mathrm{i}}\|X(\tau)\|^2 - \|s\|\|\tau_i\| &\geq 0. \end{aligned} \tag{14}$$

• If the interaction force $\|\tau_\mathrm{i}\| \neq 0$, according to the uniformly ultimately bounded (UUB) stability theory, it follows that $\|s\|^2$ and $\|\mathrm{vec}(K(t))\|^2$ go to the bounded set Ω which is defined as follows:

$$\Omega = \left\{ \|s\|^2, \|\mathrm{vec}(K(t))\|^2 \middle| \frac{4(1-w_\mathrm{i})^2\overline{\lambda}_K^2(\|s\| - \frac{1}{2(1-w_\mathrm{i})\overline{\lambda}_K}\|\tau_\mathrm{i}\|)^2}{\|\tau_\mathrm{i}\|^2} \right.$$

$$+\frac{4\gamma\overline{\lambda}_K w_{\mathrm{i}}\|\mathrm{vec}(K(t))\|^2}{\|\tau_{\mathrm{i}}\|^2}\le 1\Big\}. \tag{15}$$

• If the interaction force $\|\tau_{\mathrm{i}}\| = 0$, the function eq. (14) holds and $\delta V \le 0$ always holds, which means eq. (4) can be minimized.

Remark 2. It is obvious that eq. (15) follows the form of an ellipse in the first quadrant:

$$\frac{(x-h)^2}{a}+\frac{(y-k)^2}{b}=1, x\ge 0, y\ge 0, \tag{16}$$

where $h = 1/(2(1-w_{\mathrm{i}})\overline{\lambda}_K)\|\tau_{\mathrm{i}}\|$, $k = 0$, $a = \|\tau_{\mathrm{i}}\|^2/(4(1-w_{\mathrm{i}})^2\overline{\lambda}_K^2)$ and $b = \|\tau_{\mathrm{i}}\|^2/(4\gamma\overline{\lambda}_K w_{\mathrm{i}})$. From eq. (16), it can be concluded that the upper limits of x and y are $\sqrt{h}+a$ and $\sqrt{k}+b$, respectively. Note that as w_{i} increases, h and a increase while b decreases. It means that the interaction factor w_{i} can affect the shape of the ultimate upper limits of $\|s\|^2$ and $\|\mathrm{vec}(K(t))\|^2$. When the patient has a stronger interaction intention, then w_{i} increases. As a result, the upper bound of tracking error $\|s\|^2$ is increased to allow a larger tracking error and the upper bound of $\|\mathrm{vec}(K(t))\|^2$ is decreased to generate a lower stiff. Figure 2 is given to show the change of eq. (15) caused by different w_{i}.

Remark 3. According to eqs. (15) and (16), the forgetting factor γ is closely related to the ultimate bound of the stiffness matrix $K(t)$. A larger γ leads to a lower ultimate upper bound of $K(t)$. In this way, the robot behaves more "compliant", which is beneficial to the patient's active rehabilitation training. However, a large γ can cause the vibration of $K(t)$ by eq. (5), which results in a worse transient process of $K(t)$ and may cause the un-safety during the rehabilitation training. Therefore, there is a selection trade-off for γ. In practice, the forgetting factor γ should be initially set to be a small value, and then be gradually increased meanwhile the vibration of $K(t)$ is avoided. By this trial-and-error process, the forgetting factor γ can be determined.

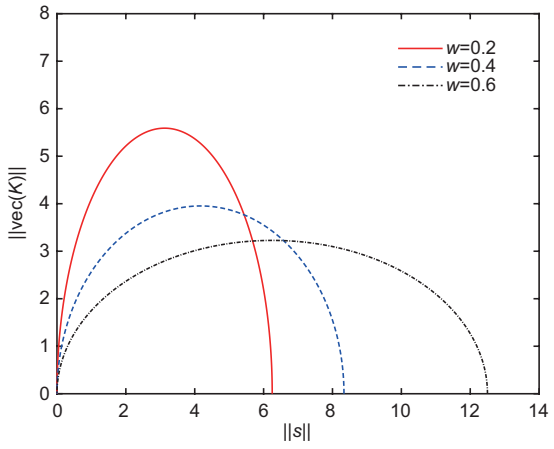

Figure 2 (Color online) Curve of eq. (15) with different ω_{i}.

2.3 Interaction force estimation

The controller designed in the above section does not consider the effect of the interaction force τ_{i}. If this force can be considered in the controller, a better control performance can be achieved. In this paper, a force estimation based on the generalized momentum method is used to estimate the interaction force [34]. First, the generalized momentum can be defined as

$$p = M(q)\dot{q}. \tag{17}$$

Taking eq. (17) into eq. (1), it generates that

$$\dot{p} = C^{\mathrm{T}}(q,\dot{q})\dot{q} + \tau_{\mathrm{c}} - G(q) - \tau_{\mathrm{i}} = u - \tau_{\mathrm{i}}, \tag{18}$$

where u is defined as $u = C^{\mathrm{T}}(q,\dot{q})\dot{q}+\tau_{\mathrm{c}}$. The interaction force τ_{i} can be modeled as follows:

$$\dot{\tau}_{\mathrm{i}} = A\tau_{\mathrm{i}} + w_\tau, \tag{19}$$

where w_τ denotes the uncertainty and satisfies $w_\tau \sim N(0, Q_\tau)$. A is the constant gain matrix. Combining eq. (18) and eq. (19) has

$$\begin{aligned}&\begin{bmatrix}\dot{p}\\ \dot{\tau}_{\mathrm{i}}\end{bmatrix} = \begin{bmatrix}0_n & -I_n\\ 0_n & A\end{bmatrix}\begin{bmatrix}p\\ \tau_{\mathrm{i}}\end{bmatrix} + \begin{bmatrix}I_n\\ 0_n\end{bmatrix}u + \begin{bmatrix}0\\ w_\tau\end{bmatrix},\\ &y = \begin{bmatrix}I_n & 0_n\end{bmatrix}\begin{bmatrix}p\\ \tau_{\mathrm{i}}\end{bmatrix} + v,\end{aligned} \tag{20}$$

where v is the measurement noise and satisfies $v \sim N(0, R_{\mathrm{e}})$. Let $x = [p^{\mathrm{T}}, \tau_{\mathrm{i}}^{\mathrm{T}}]^{\mathrm{T}}$, $A_{\mathrm{e}} = [0_n, -I_n; 0_n, A]$, $B_{\mathrm{e}} = [I_n, 0_n]^{\mathrm{T}}$, and $C_{\mathrm{e}} = [I_n, 0_n]$. Define $\hat{x}$ and $\hat{y}$ as the estimated values of x and y. Then a state observer is constructed as follows:

$$\begin{aligned}&\dot{\hat{x}} = A_{\mathrm{e}}\hat{x} + B_{\mathrm{e}}u + L(y-\hat{y}),\\ &\hat{y} = C_e\hat{x},\end{aligned} \tag{21}$$

where L is designed by

$$L = PC_{\mathrm{e}}^T R_{\mathrm{e}}^{-1}, \tag{22}$$

where P is the solution of the following algebraic Riccati equation:

$$A_eP + PA_{\mathrm{e}}^{\mathrm{T}} - PC_{\mathrm{e}}^T R_{\mathrm{e}}^{-1}C_{\mathrm{e}}P + Q_{\mathrm{e}} = 0, \tag{23}$$

where $Q_{\mathrm{e}} = \mathrm{diag}([0, Q_\tau])$ denotes the uncertainty of the state. From the definition of $x(t)$, the estimated value of the interaction force τ_{i} is

$$\hat{\tau}_{\mathrm{i}} = \begin{bmatrix}0&0&1&0\\ 0&0&0&1\end{bmatrix}\hat{x}. \tag{24}$$

Since the linear augmented system defined by eq. (20) is observable and the observer defined by eq. (21) is a continuous-time Kalman filter, by the same analysis technique in ref. [35], the estimation error of the interaction force $\widetilde{\tau}_{\mathrm{i}} = \tau_{\mathrm{i}} - \hat{\tau}_{\mathrm{i}}$ is bounded.

Using the above force estimation, a controller with the compensation of the interaction force is given as follows:

$$\tau_u = -K(t)s + M(q)(\ddot{q}_{\mathrm{d}} - \dot{q}_{\mathrm{e}}) + C(q,\dot{q})(\dot{q}_{\mathrm{d}} - q_{\mathrm{e}}) + G(q) - \hat{\tau}_{\mathrm{i}}. \tag{25}$$

Taking eq. (25) into eq. (1) leads to

$$\begin{aligned} M(q)\ddot{q} + C(q,\dot{q})\dot{q} + G(q) &= -K(t)s + M(q)(\ddot{q}_{\mathrm{d}} - \dot{q}_{\mathrm{e}}) \\ &\quad + C(q,\dot{q})(\dot{q}_{\mathrm{d}} - q_{\mathrm{e}}) + G(q) - \hat{\tau}_{\mathrm{i}} + \tau_{\mathrm{i}}, \\ M(q)\dot{s} + C(q,\dot{q})s + K(t)s &= \widetilde{\tau}_{\mathrm{i}}. \end{aligned} \tag{26}$$

Theorem 2. By adopting the iterative updating law defined by eq. (5) and the controller defined by eq. (25), the first-order difference of the overall cost function satisfies that $\sigma V(t) \le 0$ until $\|s\|$ and $\|\mathrm{vec}(K(t))\|$ finally go to the bounded set defined in the following proof. This indicates that the cost function can be reduced by eqs. (4) and (25).

Proof. Set the Lyapunov candidate to be $V = V_{\mathrm{c}} + V_p$ as the one defined by eq. (4). The calculation of δV_{c} is the same as the one defined by eq. (12).

The time-derivative of $V_p(t)$ is

$$\begin{aligned} \dot{V}_p &= s^{\mathrm{T}} M(q)\dot{s} + \frac{1}{2}s^{\mathrm{T}}\dot{M}(q)s \\ &= s^{\mathrm{T}}[-C(q,\dot{q})s - K(t)s + \widetilde{\tau}_{\mathrm{i}}] + \frac{1}{2}s^{\mathrm{T}}\dot{M}(q)s \\ &= -s^{\mathrm{T}}K(t)s + s^{\mathrm{T}}\widetilde{\tau}_{\mathrm{i}}. \end{aligned} \tag{27}$$

Integrating eq. (27) from $(t-T)$ to t, the first-order difference of $V_p(t)$ is

$$\delta V_p = \int_{t-T}^{t} \dot{V}_p(\tau)\mathrm{d}\tau = -\int_{t-T}^{t} [s^{\mathrm{T}}K(t)s - s^{\mathrm{T}}\widetilde{\tau}_i]\mathrm{d}\tau. \tag{28}$$

According to eq. (28) and eq. (12), δV is given as

$$\begin{aligned} \delta V = &-\int_{t-T}^{t}\left[(1-w_{\mathrm{i}})s^{\mathrm{T}}Ks + \frac{\gamma}{1-w_{\mathrm{i}}}X(\tau)^{\mathrm{T}}X(\tau) - s^{\mathrm{T}}\widetilde{\tau}_{\mathrm{i}}\right]\mathrm{d}\tau \\ &-\frac{1}{2}\int_{t-T}^{t}\delta X(\tau)^{\mathrm{T}}\delta X(\tau)\mathrm{d}\tau. \end{aligned} \tag{29}$$

Following the similar procedure from eq. (13) to eq. (15), it can be obtained that

$$\begin{aligned} \bar{\Omega} = \Bigg\{ &\|s\|^2, \|\mathrm{vec}(K(t))\|^2 \Bigg| \frac{4(1-w_{\mathrm{i}})^2\overline{\lambda}_K^2(\|s\| - \frac{1}{2(1-w_{\mathrm{i}})\overline{\lambda}_K}\|\widetilde{\tau}_i\|)^2}{\|\widetilde{\tau}_i\|^2} \\ &+ \frac{4\gamma\overline{\lambda}_K w_{\mathrm{i}}\|\mathrm{vec}(K(t))\|^2}{\|\widetilde{\tau}_i\|^2} \le 1 \Bigg\}, \end{aligned} \tag{30}$$

where $\bar{\Omega}$ is the set which $\|s\|^2$ and $\|\mathrm{vec}(K(t))\|^2$ ultimately go into. If the estimation error of the interaction force is $\|\widetilde{\tau}_{\mathrm{i}}\| = 0$, the function eq. (29) is always nonnegative, which implies the minimization of eq. (4).

From the above analysis, the set $\bar{\Omega}$ is affected by the interaction factor w_{i} and the estimation error $\widetilde{\tau}_{\mathrm{i}}$. The adjustment of w_{i} can affect whether the whole system is compliant to the patient. Eq. (30) also follows the form of the eclipse eq. (16) where $h = 1/(2(1-w_{\mathrm{i}})\overline{\lambda}_K)\|\widetilde{\tau}_{\mathrm{i}}\|$, $k = 0$, $a = \|\widetilde{\tau}_{\mathrm{i}}\|^2/(4(1-w_{\mathrm{i}})^2\overline{\lambda}_K^2)$ and $b = \|\widetilde{\tau}_{\mathrm{i}}\|^2/(4\gamma\overline{\lambda}_K w_{\mathrm{i}})$. Consider the fact that the estimation error $\|\widetilde{\tau}_{\mathrm{i}}\|$ is usually smaller than $\|\tau_{\mathrm{i}}\|$ in practice. This leads to the smaller $\sqrt{h} + a$ and $\sqrt{k} + b$. Therefore, the ultimate tracking error and the stiff parameters are smaller which is beneficial for the patient's rehabilitation training.

Remark 4. According to the Brunnstrom rehabilitation assessment theory, the rehabilitation process of the post-stroke patients can be divided into six phases: (1) flaccidity; (2) synergies (some spasticity); (3) marked spasticity; (4) out of synergy (less spasticity); (5) selective control of movement; and (6) isolated/coordinated movement. During different rehabilitation phases, different treatments should be adopted. Usually, the physical therapy (PT) treatment is adopted during the first two phases ("flaccidity" and "synergies") and the occupational therapy (OT) treatment is adopted in the last two phases ("selective control of movement" and "isolated/coordinated movement"). For the phases of "marked spasticity" and "out of synergy", some special treatments are applied to avoid the muscle spasticity.

According to the "assist-as-needed" feature of the proposed controller, it can be applied in both the PT treatment and the OT treatment. During the PT treatment, the patient's muscle lacks of the motion ability. By selecting a small interaction factor w_{i}, the ultimate upper bound of the tracking error becomes smaller and the patient passively follows the robot's motion. During the OT treatment, the patient has partially recovered his/her motion ability. The robot should behave compliantly to stimulate the patient's own motion by setting the interaction factor w_{i} close to one.

3 Simulation results

The rehabilitation robot model is assumed to be a two-link revolute joint robot that can represent the finger rehabilitation robot shown in Figure 3. The details of the robot's model are listed as follows [36]:

$$\begin{bmatrix} M_{11}(q) & M_{12}(q) \\ M_{21}(q) & M_{22}(q) \end{bmatrix}\ddot{q}_{\mathrm{i}} + \begin{bmatrix} C_{11}(q,\dot{q}) & C_{12}(q,\dot{q}) \\ C_{21}(q,\dot{q}) & C_{22}(q,\dot{q}) \end{bmatrix}\dot{q}_{\mathrm{i}} + \begin{bmatrix} g_1(q) \\ g_2(q) \end{bmatrix} = \tau_u + \tau_{\mathrm{i}}.$$

All elements of $M(q)$, $C(q,\dot{q})$ and g are listed as follows:

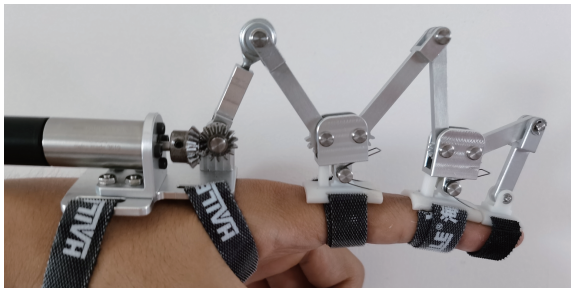

Figure 3 (Color online) The finger rehabilitation robot prototype.

$$M_{11}(q) = m_1 l_{c1}^2 + m_2[l_1^2 + l_{c2}^2 + 2l_1 l_{c2}\cos(q_2)] + I_1 + I_2,$$
$$M_{12}(q) = M_{21}(q) = m_2[l_{c2}^2 + l_1 l_{c2}\cos(q_2)] + I_2,$$
$$M_{22}(q) = m_2 l_{c2}^2 + I_2,$$
$$C_{11}(q,\dot{q}) = -m_2 l_1 l_{c2}\sin(q_2)\dot{q}_2,$$
$$C_{12}(q,\dot{q}) = -m_2 l_1 l_{c2}\sin(q_2)(\dot{q}_1 + \dot{q}_2),$$
$$C_{21}(q,\dot{q}) = m_2 l_1 l_{c2}\sin(q_2)\dot{q}_1,$$
$$C_{22}(q,\dot{q}) = 0,$$
$$g_1(q) = (m_1 l_{c1} + m_2 l_1)g\sin(q_1) + m_2 l_{c2} g\sin(q_1 + q_2),$$
$$g_2(q) = m_2 l_{c2} g\sin(q_1 + q_2).$$

The physical parameters of the robot are chosen as follows: $m_1 = 1.0$ kg, $m_2 = 0.5$ kg, $l_1 = 1.0$ m, $l_2 = 0.6$ m, $l_{c1} = 0.5$ m, $l_{c2} = 0.3$ m, $J_1 = 0.2083$ kg/m^2, $J_2 = 0.0540$ kg/m^2, and $g = 9.8$ m/s^2. The initial states of the robot are chosen as $q(0) = [3,2]^{\mathrm{T}}$ rad and $\dot{q}(0) = [1,0]^{\mathrm{T}}$ rad/s. The goal states of the robot are chosen as $q_{\mathrm{d}}(t) \equiv [1,0]^{\mathrm{T}}$ rad, $\dot{q}_{\mathrm{d}}(t) \equiv [0,0]^{\mathrm{T}}$ rad/s.

In this simulation section, four groups of simulations are conducted to show the effectiveness of the proposed algorithm. The total iteration number is 4. The robot's torque controller used in Sects. 3.1, 3.2, and 3.4 takes the form defined by eq. (3). In Sect. 3.3, the robot's torque controller is based on the force estimation, which is defined by eq. (25). The initial stiffness matrix is chosen as $K(0) = [0,0;0,0]$. The new stiffness matrix is updated by the proposed iterative updating law defined by eq. (7). The forgetting factor in eq. (7) is set to be $\gamma = 0.01$. All simulation examples are conducted by using the "ode4" method of Matlab 9.7 on the platform of CPU Intel Core i5-8300H, Windows 10.

3.1 Effectiveness of the interaction factor

To verify the proposition that the interaction factor w_{i} can affect the ultimate bounded set of the tracking error and the stiffness parameters, two types of interaction factors are chosen in Figure 4. The interaction force τ_{i} in this simulation is assumed to be $\tau_{\mathrm{i}} = [10,0]^{\mathrm{T}}$N. In Figure 4, dotted lines denote the results with $w_{\mathrm{i}} = 0.4$, solid lines denote the results with $w_{\mathrm{i}} = 0.6$, and different lines denote different iterative times. Figure 4(a) shows the filtered tracking errors s under the controller defined by eq. (3). Figure 4(b) shows the profiles of the robot's joint angle q under the controller defined by eq. (3). Figure 4(c) shows the mean values of every element of the stiffness matrix K under the controller defined by eq. (3). With the interaction factor being $w_{\mathrm{i}} = 0.4$, the tracking errors of four iteration are $[1.513,0]^{\mathrm{T}}$, $[1.072,0]^{\mathrm{T}}$, $[0.896,0]^{\mathrm{T}}$

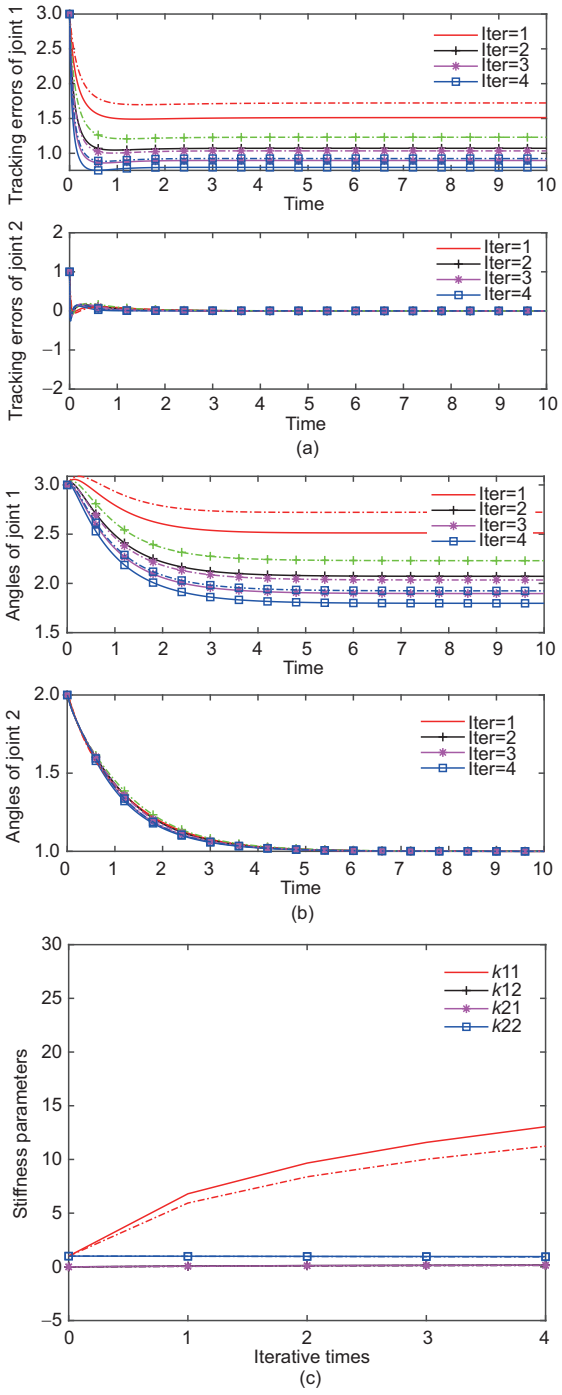

Figure 4 (Color online) Simulation results under the controller defined by eq. (3) with two different interaction factors. (a) Tracking errors; (b) joint angles; (c) stiffness parameters.

and $[0.798, 0]^{\mathrm{T}}$rad, and the final average stiffness matrix after four iterations is $K(t) = [13.048, 0.155; 0.155, 0.956]$. With the interaction factor being $w_{\mathrm{i}} = 0.6$, the tracking errors of four iteration are $[1.723, 0]^{\mathrm{T}}$, $[1.231, 0]^{\mathrm{T}}$, $[1.034, 0]^{\mathrm{T}}$ and $[0.924, 0]^{\mathrm{T}}$rad, and the final average stiffness matrix after four iterations is $[11.237, 0.137; 0.137, 0.922]$. From the above results, it is obvious that a larger w_{i} can lead to the larger allowable tracking errors and the smaller stiffness parameters.

3.2 Test with the time-varying interaction force

To show the controller defined by eq. (3) can achieve the assist-as-needed control, the interaction force is further assumed to be time-varying and can increase as long as the iteration. In this simulation, the interaction force satisfies the following form:

$$\tau_{\mathrm{i}}(t) = \begin{cases} 0.5(\lfloor t/T \rfloor + 1)t + 0.5, \\ \qquad \text{when } 0 \le \mathrm{mod}(t/T) < 5, \\ -0.5(\lfloor t/T \rfloor + 1)(t-5) + 2.5(\lfloor t/T \rfloor + 1) + 0.5, \\ \qquad \text{when } 5 \le \mathrm{mod}(t/T) < 10, \end{cases}$$

where $T = 10$ s, $t \in (0, 4T)$ is the simulation time and $\mathrm{mod}(\cdot)$ denotes the remainder operator. The mean values of interaction forces during four iterations are $[2.988, 0]^{\mathrm{T}}$, $[4.231, 0]^{\mathrm{T}}$ $[5.475, 0]^{\mathrm{T}}$ and $[6.719, 0]^{\mathrm{T}}$N. The interaction force is increasing because of the increase of the motion intention of the patient. The simulation results are shown in Figure 5. With the controller defined by eq. (3), the tracking errors of four iterations are $[0.759, 0.111]^{\mathrm{T}}$, $[0.460, 0.048]^{\mathrm{T}}$, $[0.865, 0.151]^{\mathrm{T}}$ and $[1.167, 0.247]^{\mathrm{T}}$rad, and the final average stiffness matrix after four iterations is $[4.333, 0.096, 0.096, 0.226]$. It is obvious that the stiffness parameters decrease when the mean value of the interaction force exceeds τ^*, which means the system can behave more compliant if the patient has the strong motion intention.

3.3 Effectiveness of the force estimation

To test the effectiveness of the interaction force estimation, two groups of simulation studies are made in Figure 6. The interaction force in this simulation is $\tau_{\mathrm{i}} = [10, 0]^{\mathrm{T}}$N. In Figure 6, dotted lines denote the results under the controller defined by eq. (25), solid lines denote the results under the controller defined by eq. (3), and different lines denote different iteration times. Figure 6(a) shows the tracking errors s under the controller defined by eq. (3). Figure 6(b) shows the robot's joint profile q. Figure 6(c) shows the mean values of four elements of the stiffness matrix K under the controller defined by eq. (3). With the controller defined by eq. (3), the tracking errors of four iterations are $[1.513, 0]^{\mathrm{T}}$, $[1.072, 0]^{\mathrm{T}}$, $[0.896, 0]^{\mathrm{T}}$ and $[0.798, 0]^{\mathrm{T}}$rad, and the ultimate average stiffness matrix after four iterations is $[13.048, 0.155; 0.155, 0.956]$. With the controller defined by eq. (25), the tracking errors of four iteration are $[0.094, 0]^{\mathrm{T}}$, $[0.032, 0]^{\mathrm{T}}$, $[0.013, 0]^{\mathrm{T}}$ and $[0.002, 0]^{\mathrm{T}}$rad, and the ultimate average stiffness matrix after four iterations is $[2.923, 0.3034; 0.304, 1.076]$. From the above results, it is obvious that the force estimation can bring a better control performance

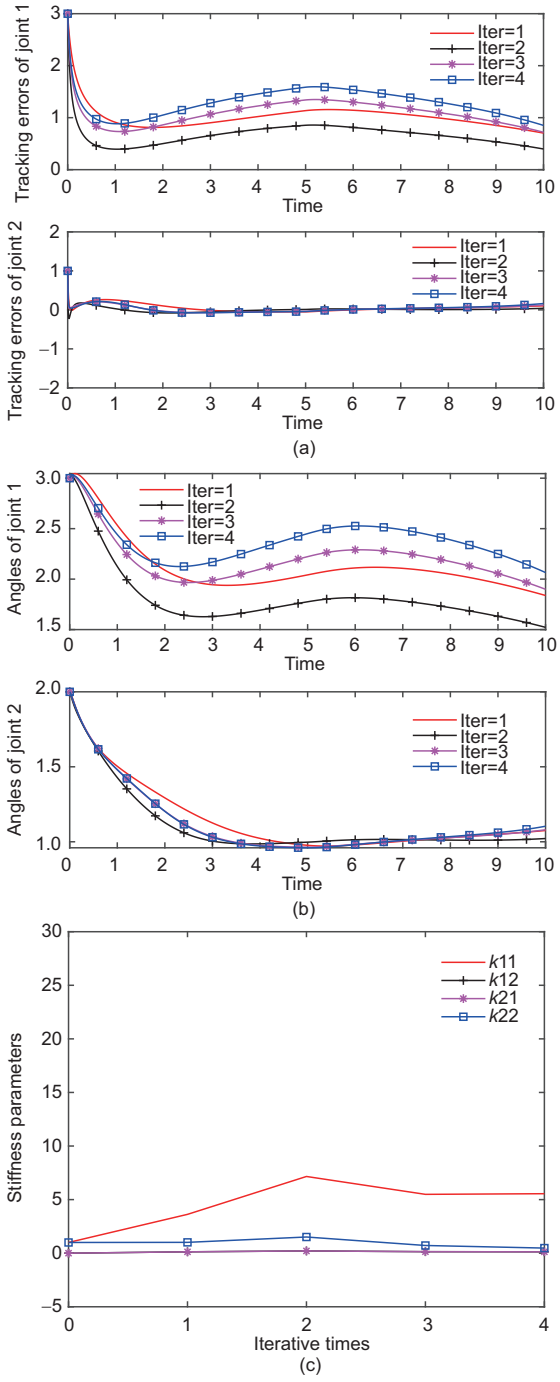

Figure 5 (Color online) Simulation results under the controller defined by eq. (3) with the time-varying interaction force. (a) Tracking errors; (b) joint angles; (c) stiffness parameters.

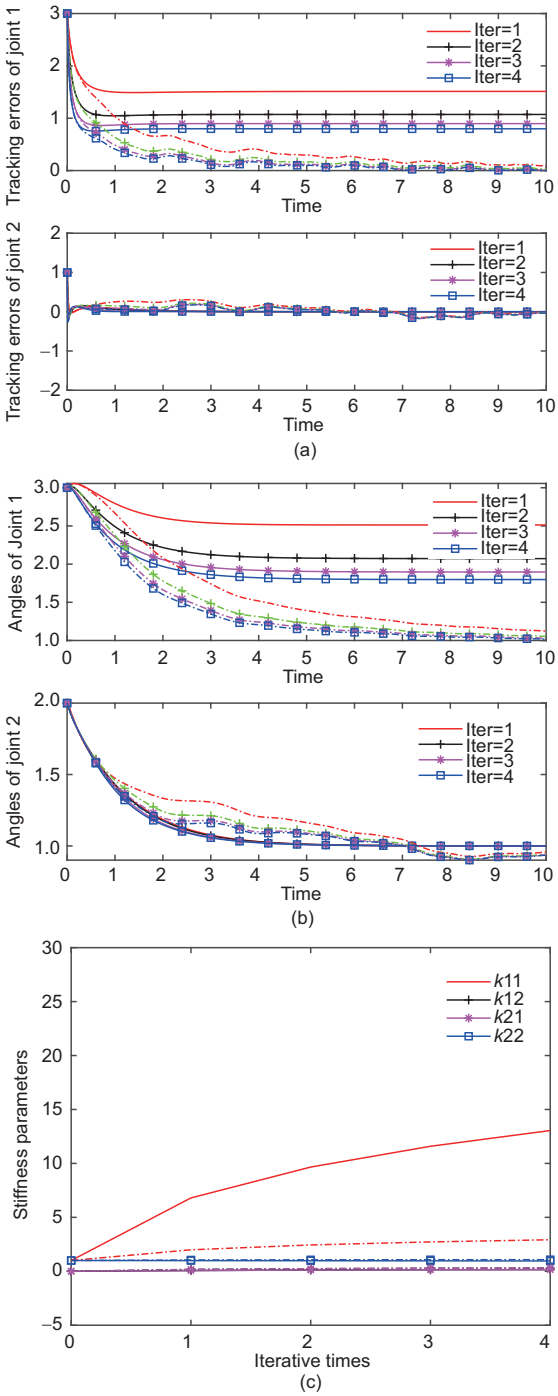

Figure 6 (Color online) Simulation results under the controller defined by eq. (25) and the controller defined by eq. (3). (a) Tracking errors; (b) joint angles; (c) stiffness parameters.

because of the lower allowable tracking errors and the lower stiffness parameters.

3.4 Comparison with the minimal assist-as-needed controller

Compared with the minimal assist-as-needed controller proposed in ref. [28], the algorithm designed in this paper can achieve a better performance. For guaranteeing the fairness of this comparison, the state observer used in ref. [28] is replaced by the true state value as the one used in this paper. Then the minimal assist-as-needed controller is listed as follows:

$$\begin{aligned}
&\tau_u = M(q)(\ddot{q}_\mathrm{d} + \dot{q}_\mathrm{e}) + C(q,\dot{q})(\dot{q}_\mathrm{d} + q_\mathrm{e}) + g(q) - K_k s,\\
&K_k = (1 + x_{k-1})K_{k-1},\\
&x_{k-1} = \frac{\overline{r}_{k-1} - r^*}{r^*}\left(\frac{\|\overline{r}_{k-1} - r^*\|}{\|\overline{r}_{k-2} - r^*\|}\right)^{\mathrm{sign}(r^* - \hat{r}_{k-1})},
\end{aligned} \tag{31}$$

where r^* denotes the allowable motion error, and $\overline{r}_{k-1}$ denotes the mean value of the motion errors in the $(k-1)$th experiment. By replacing $\overline{\tau}_{k-1}$ and τ^* with $\overline{r}_{k-1}$ and r^*, respectively, the interaction factor w_i in eq. (7) can also be constructed by the motion error. In this simulation, r^* is chosen as $r^* = 0.8$. Two initial stiffness matrices are both set to be the unit matrix.

In Figure 7, the dotted line represents the results under the controller defined by eq. (31), and the solid line represents the results under the controller defined by eq. (3). With the controller defined by eq. (3), the tracking errors of four iterations are $[1.513, 0]^\mathrm{T}$, $[1.666, 0]^\mathrm{T}$, $[1.348, 0]^\mathrm{T}$ and $[1.131, 0]^\mathrm{T}$rad, and the final average stiffness matrix after four iterations is $[9.141, 0.117; 0.117, 0.406]$. With the controller defined by eq. (31), the tracking errors of four iterations are $[6.832, -0.640]^\mathrm{T}$, $[0.966, 0]^\mathrm{T}$, $[0.966, 0]^\mathrm{T}$ and $[0.800, 0]^\mathrm{T}$rad, and the final average stiffness matrix after four iterations is $[12.501, 0; 0, 12.501]$. It is clear that when the patient applies the same interaction force, the system under the controller defined by eq. (3) behaves more compliantly, and it is more helpful to the active participation of the patient.

4 Conclusions

This paper studies a novel assist-as-needed controller for the interaction control between the rehabilitation robot and the patient. This controller includes an adjustable stiffness matrix whose iterative updating law is designed to reduce the cost function composed of the tracking error and the stiffness parameters. The cost function includes an interaction factor reflecting the patient's motion intention. When the patient applies sufficiently large interaction force, this interaction factor becomes larger, and then the allowable tracking error of the robot system becomes larger and the stiffness parameter becomes smaller. Furthermore, a compensation of interaction force based on the force estimation is given to further improve the control performance. Finally, the Lyapunov analysis and simulation results are given to demonstrate the effectiveness of the proposed algorithm. Future work is to focus on the determination of w_i by using some motion intention recognition

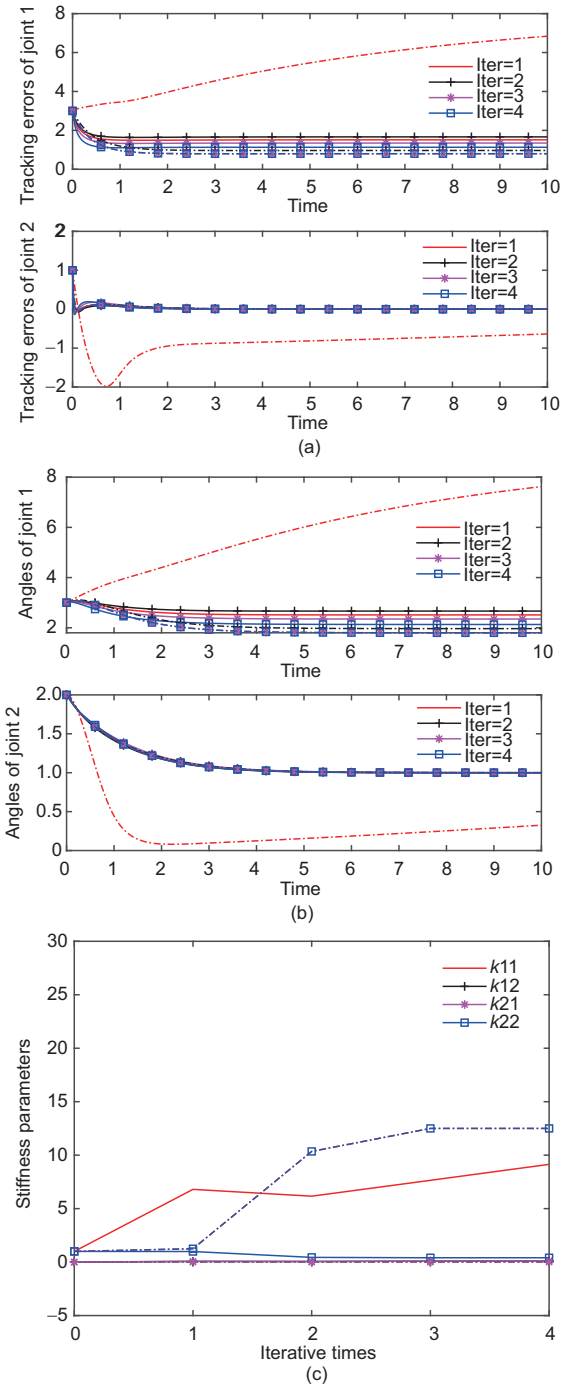

Figure 7 (Color online) Simulation results under the controller eq. (31) and eq. (3). (a) Tracking errors; (b) joint angles; (c) stiffness parameters.

algorithms (based on the patient's physiological and kinematic cues) and to conduct the corresponding physical verification experiments.

This work was supported by the National Natural Science Foundation of China (Grant Nos. U1913209, 61873268, 62025307), and the Beijing Municipal Natural Science Foundation (Grant No. JQ19020).

1 Wang L D, Mao Q A, Zhang Z J. Report on the Chinese Stroke Prevention (2018). Beijing: People's Medical Publishing House, 2018
2 Liang X, Wang W, Hou Z, et al. Interactive control methods for rehabilitation robot. Sci Sin-Inf, 2018, 48: 24–46
3 Ghannadi B, Mehrabi N, Razavian R S, et al. Nonlinear model predictive control of an upper extremity rehabilitation robot using a two-dimensional human-robot interaction model. In: Proceedings of IEEE International Conference on Intelligent Robots and Systems. Vancouver, 2017. 502–507
4 Ma Z, Ben-Tzvi P, Danoff J. Hand Rehabilitation learning system with an exoskeleton robotic glove. IEEE Trans Neural Syst Rehabil Eng, 2016, 24: 1323–1332
5 Zhang F, Hou Z G, Cheng L, et al. iLeg—A lower limb rehabilitation robot: A proof of concept. IEEE Trans Human-Mach Syst, 2016, 46: 761–768
6 Girone M, Burdea G, Bouzit M. "Rutgers Ankle" orthopedic rehabilitation interface. In: Proceedings of the ASME International Mechanical Engineering Congress and Exposition. Nashville, 1999. 305–312
7 Saglia J A, Tsagarakis N G, Dai J S, et al. Control strategies for patient-assisted training using the ankle rehabilitation robot (ARBOT). IEEE/ASME Trans Mechatron, 2013, 18: 1799–1808
8 Ayas M S, Altas I H, Sahin E. Fractional order based trajectory tracking control of an ankle rehabilitation robot. Trans Institute Measurement Control, 2018, 40: 550–564
9 Ayas M S, Altas I H. Designing and implementing a plug-in type repetitive controller for a redundantly actuated ankle rehabilitation robot. Proc Institution Mech Engineers Part I-J Syst Control Eng, 2018, 232: 592–607
10 Wei H X, Li H Y, Tan J D, et al. Self-assembly control and experiments in swarm modular robots. Sci China Tech Sci, 2012, 55: 1118–1131
11 Taheri A, Orangi S. A novel miniature virus-inspired swimming robot for biomedical applications. Sci China Tech Sci, 2010, 53: 2883–2895
12 Guo S P, Li D X, Meng Y H, et al. Task space control of free-floating space robots using constrained adaptive RBF-NTSM. Sci China Tech Sci, 2014, 57: 828–837
13 Yu J Z, Wen L, Ren Z Y. A survey on fabrication, control, and hydrodynamic function of biomimetic robotic fish. Sci China Tech Sci, 2017, 60: 1365–1380
14 Sha Sadeghi M, Momeni H R. A new impedance and robust adaptive inverse control approach for a teleoperation system with varying time delay. Sci China Ser E-Technol Sci, 2009, 52: 2629–2643
15 Mo Y, Jiang Z H, Li H, et al. A kind of biomimetic control method to anthropomorphize a redundant manipulator for complex tasks. Sci China Tech Sci, 2020, 63: 14–24
16 Hogan N. Impedance control: An approach to manipulation. In: Proceedings of American Control Conference. San Diego, 1984
17 Ott C, Mukherjee R, Nakamura Y. Unified impedance and admittance control, In: Proceedings of IEEE International Conference on Robotics and Automation. Anchorage, 2010. 554–561
18 Sun T, Cheng L, Peng L, et al. Learning impedance control of robots with enhanced transient and steady-state control performances. Sci China Inf Sci, 2020, 63: 192205
19 Cui J, Lai M, Chu Z, et al. Experiment on impedance adaptation of under-actuated gripper using tactile array under unknown environment. Sci China Inf Sci, 2018, 61: 122202
20 Sun T, Peng L, Cheng L, et al. Composite learning enhanced robot impedance control. IEEE Trans Neural Netw Learning Syst, 2020, 31: 1052–1059
21 Ayas M S, Altas I H. Fuzzy logic based adaptive admittance control of a redundantly actuated ankle rehabilitation robot. Control Eng Practice, 2017, 59: 44–54
22 Bien Z, Xu J X. Iterative Learning Control: Analysis, Design, Integration and Applications. Norwell: Kluwer, 1998
23 Yang C, Ganesh G, Haddadin S, et al. Human-like adaptation of force and impedance in stable and unstable interactions. IEEE Trans Robot, 2011, 27: 918–930

24 Li Y, Ganesh G, Jarrasse N, et al. Force, impedance, and trajectory learning for contact tooling and haptic identification. IEEE Trans Robot, 2018, 34: 1170–1182

25 Zeng C, Yang C, Chen Z. Bio-inspired robotic impedance adaptation for human-robot collaborative tasks. Sci China Inf Sci, 2020, 63: 170201

26 Zhang J, Cheah C C. Passivity and stability of human-robot interaction control for upper-limb rehabilitation robots. IEEE Trans Robot, 2015, 31: 233–245

27 Jenkins W M, Merzenich M M. Reorganization of neurocortical representations after brain injury: A neurophysiological model of the bases of recovery from stroke. Progress in Brain Research, 1987, 71: 249–266

28 Pehlivan A U, Losey D P, OMalley M K. Minimal assist-as-needed controller for upper limb robotic rehabilitation. IEEE Trans Robot, 2016, 32: 113–124

29 Li X, Pan Y, Chen G, et al. Adaptive Human-robot interaction control for robots driven by series elastic actuators. IEEE Trans Robot, 2017, 33: 169–182

30 Li X, Liu Y H, Yu H. Iterative learning impedance control for rehabilitation robots driven by series elastic actuators. Automatica, 2018, 90: 1–7

31 Wang Y X, Liu H, Leng D L, et al. New advances in EMG control methods of anthropomorphic prosthetic hand. Sci China Tech Sci, 2017, 60: 1978–1979

32 Spong M W, Hutchinson S, Vidyasagar M. Robot Modeling and Control. New York: John Wiley & Sons Inc, 2006

33 Slotine J E, Li W. Applied Nonlinear Control. Englewood Cliff: Prentice-Hall, 1991

34 Yang C, Peng G, Cheng L, et al. Force sensorless admittance control for teleoperation of uncertain robot manipulator using neural networks. IEEE Trans Syst Man Cybern Syst, 2019, 1–11

35 Wahrburg A, Morara E, Cesari G, et al. Cartesian contact force estimation for robotic manipulators using Kalman filters and the generalized momentum. In: Proceedings of IEEE International Conference on Automation Science and Engineering. Gothenburg, 2015

36 Kelly R, Davila V S, Perez J A. Control of robot manipulators in joint space. London: Springer Science & Business Media, 2006